New Insights into the Relationship between Ion-Pair Binding Energy and Thermodynamic and Transport Properties of Ionic Liquids†

Uditha L. Bernard, Ekaterina I. Izgorodina,* and Douglas R. MacFarlane

School of Chemistry, Monash University, Clayton, Victoria 3800, Australia

Received: May 27, 2010

To aid in the design of novel task-specific ionic liquids (ILs), this study investigates the relationship between trends in ion-pair binding energy (IPBE) and trends in thermodynamic and transport properties of ILs. Unlike previous studies, this study considers the two major components of the IPBE, namely, the electrostatic and dispersion interactions, and suggests how these components relate to melting point and transport properties such as conductivity and viscosity. A range of *N*-methyl-*N*-alkylpyrrolidinium and *N*-methyl-*N*-alkylimidazolium-based salts paired with Br^-, BF_4^-, PF_6^-, $N(CN)_2^-$, $N(SO_2CF_3)_2^-$ (also known as NTf_2^-), mesylate, and tosylate anions were studied. It was found that the ratio of total IPBE to its dispersion component correlates well with melting point, whereas the dispersion component of the IPBE correlates well with conductivity and viscosity.

Introduction

Ionic liquids (ILs) are low melting point salts, which, by definition, melt below 100 °C. They have been found to be useful as solvents in organic synthesis and extraction processes,[1−3] and it is well known that the performance of energy-generating electrochemical devices may be improved by replacing traditional electrolytes with ILs.[4−6] By altering the cations and anions that form the IL, there is potential to tailor the properties of the IL to better meet the needs of particular applications. Theoretical methods to predict the properties of proposed cation−anion combinations before synthesis are useful in designing novel ILs. In particular, knowledge of the thermodynamic and transport properties of an IL is of importance in assessing its suitability as an electrolyte in lithium batteries, solar, and fuel cells. Several different computational approaches have been taken to facilitate the prediction of thermodynamic and transport properties of ILs. These approaches are briefly outlined below, before the hypotheses tested in the present study are explained.

Quantitative structure property relationship models to predict melting points[1,7−9] and transport properties[10,11] of various groups of ILs have been developed. These models are developed through a statistical analysis of the correlation between available experimental data and a range of computed properties. Each model is limited to a particular property of a particular group of ILs. In addition to quantitative estimates, these models have provided some qualitative information about the structural features of cations and anions that correlate with particular characteristics.

Classical molecular dynamics (MD) has successfully simulated various thermodynamic and transport properties of ILs.[12−18] Because classical MD uses force fields developed by parametrizing experimental data, it is unsuitable to predict properties for classes of ILs for which little or no experimental data are available.[19] Additional problems with applying standard methods to simulate the melting of ILs have been noted by Maginn, such as the slow dynamics of IL systems.[20] Classical MD simulations have, however, provided some useful insights into other properties of ILs. For example, Kelkar and Maginn[21] found that the vapor phase of ILs is likely to be predominantly made up of ion pairs and that the dispersion energy contribution to the enthalpy of vaporization is similar in magnitude to the electrostatic contribution.

Ab initio MD simulations on ILs are becoming more popular,[22,23] in which the forces are calculated using ab initio methods. Although the ab initio MD approach may in the future enable direct calculations of thermodynamic and transport properties of ILs, computational cost is still high, and it is not yet feasible to routinely perform such calculations. Therefore, currently published ab initio studies have focused on trying to relate results from gas-phase calculations on ions, ion pairs, and model systems to measured thermodynamic and transport properties of ILs.

To predict boiling point, Ludwig[24] modeled the gas-phase structure of the IL as an ion pair and the liquid phase structure as a cluster of ion pairs. Statistical thermodynamics was then used to calculate the Gibbs free energy at various temperatures. The boiling point was identified via the point at which the free energy of the gas and liquid phases was the same. Such an approach is still quite computationally expensive.

One approach to predict melting points of ILs uses the concept of proton affinity.[25] "Proton affinity", defined as the energy required for the transfer of a probe proton to an anion, represents the degree of charge delocalization on an anion. It was shown that lower proton affinities correlated with lower melting points. However, proton affinity does not provide any guidance on the effect of different cations on melting point, nor does it account for specific interactions between ions.

To account for interactions between ions, various studies have sought to correlate ion-pair binding energy (IPBE) with melting point and transport properties of ILs. Zahn et al.[26] and Turner et al.[27] found no correlation between IPBE and melting point. With respect to transport properties, Tsuzuki et al.[28] found that the IPBE did not correlate with either conductivity or ion-pair association. However, for a different class of ILs, Fraser et al.[29] found that greater (i.e., more negative) IPBE correlated with

† Part of the "Mark Ratner Festschrift".

* To whom correspondence should be addressed. E-mail: katya.izgorodina@sci.monash.edu.au.

10.1021/jp1048875
Published on Web 07/07/2010

greater deviations from the ideal line on the Walden plot that was attributed to more ion pairing.

Entropy effects may partially explain why IPBE does not always correlate with observed physical properties. A study by Hunt et al.[30] investigated why an IL, which had a weaker IPBE compared with another IL, had a higher melting point. The study found that the IL with the higher melting point had a smaller number of stable ion-pair conformations, thus suggesting that it has lower entropy. Lower entropy would favor the solid state and thus was consistent with the higher melting point. "Connectivity index", defined as the number of other cations to which each cation is connected through the anions surrounding it, has been proposed as a measure of the entropy of ILs.[31] A greater connectivity index means that there is more ordering (i.e., less entropy). Although this concept is helpful to explain trends in physical properties, working out the connectivity index requires knowledge of the condensed phase structure of the IL, and this is not always readily available.

A simpler approach to predict physical properties of ILs based on the molar volume (V_m) has been suggested by Slattery et al.[32] They found that V_m, defined as the sum of volumes of individual cations and anions comprising an ionic liquid, correlated well with both conductivity and viscosity of ILs. A previous study,[33] found that melting points predicted using the volume-based thermodynamics (VBT) method developed by Glasser and Jenkins[34] correlated well with experimental melting points. A volume-based approach, however, does not take into account interactions between ions that may influence physical properties such as $\pi-\pi$ stacking and alkyl chain interactions.

Previous studies that have investigated the relationship between trends in IPBEs and trends in thermodynamic and transport properties of ILs have not considered how different components of the IPBE such as electrostatic and dispersion forces might relate to these physical properties. Possible correlations with the melting point and the transport properties are the focus of the work reported in this article.

Melting Points

The change in Gibbs free energy of melting (or fusion) is given by

$$\Delta G_f = \Delta H_f - T\Delta S_f \quad (1)$$

where ΔH_f and ΔS_f are the enthalpy and entropy of fusion, respectively, and T is the temperature. At the melting point, $\Delta G_f = 0$. Substituting this into eq 1 and rearranging gives

$$T_m = \frac{\Delta H_f}{\Delta S_f} \quad (2)$$

where T_m is the temperature at which melting occurs. Equation 2 shows that the melting point is the ratio of the changes in enthalpy and entropy in going from the solid state to the liquid state. Simple observation of a variety of salts from complex organic salts to simple inorganic salts such as NaCl suggests that the stronger the interaction between ions in the crystal, the greater is the lattice energy (U_L) and the higher is T_m. ΔH_f is related to the change in interaction energy (per mole) on passing from the crystalline lattice to the liquid state. (Changes in other components of enthalpy such as vibrational energies are assumed to be only a small part of the total here.) In the crystalline lattice, this interaction energy is equivalent to the lattice energy that is related to the individual IPBE by geometric factors including the Madelung constant of the lattice.[35]

On melting, the energy of interactions will change as a result of changes in IPBE as average distances between ions expand slightly. Because volume changes on melting of many crystalline salts are relatively similar, this relative change in IPBE we assume to be the same for most salts. Therefore, we arrive at the following approximate expression as a means of estimating ΔH_f

$$\Delta H_f \propto \text{IPBE} \quad (3)$$

The increase in entropy that occurs upon melting arises from translational and rotational motions that are allowed by a decrease in dispersion interactions; a large gain in entropy at melting should produce a lower melting point. The rationale behind the relationship between entropy of fusion and dispersion interactions stems from the fact that the latter decrease much more rapidly with distance ($\sim 1/R^6$) than electrostatic interactions ($\sim 1/R$) and are highly directional. Hence, as ions move apart and randomize their positions on melting, the relative decrease in dispersion interactions is much greater than that in the long-range electrostatic interactions; therefore, the weakening of these short-range interactions is expected to be primarily responsible for the increase in motions of the ions.

The above contentions lead to the first hypothesis in this study that ΔH_f correlates with the total IPBE, ΔS_f correlates with the dispersion component of the IPBE, and, therefore, based on eq 2, the ratio of total IPBE to its dispersion component correlates with melting point, that is

$$T_m = f\left(\frac{\text{total IPBE}}{\text{dispersion IPBE}}\right) \quad (4)$$

This approximation can only hold for ILs whose interactions are dominated by the cation−anion interactions. It is obvious that when short-range cation−cation and anion−anion dispersion interactions dominate the lattice energy (as was seen for ILs containing cations with long alkyl chains[15]), the suggested correlation of the ratio of total IPBE to its dispersion component with melting point is not expected to hold.

Transport Properties. Given the highly directional nature of dispersion forces and their short-range nature, as mentioned above, it is likely that these present the greatest barrier to relative motions of the ions with respect to each other. Small relative displacements of ions due to random thermal motions that are the origins of the transport properties will not generate large variations in the long-range electrostatic energy because the latter changes very slowly with interionic distance and is a non-directional force. Dispersion interactions are much shorter-range because these rely on instantaneous dipole moments created in nearby electron clouds; therefore, the motion of the ions may diminish these interactions quite substantially. Therefore, the second hypothesis that we test in this study is that the dispersion part of the IPBE correlates with transport properties such as conductivity and viscosity.

The present study investigates how the two major components of the IPBE, namely, the electrostatic and dispersion components, relate to the melting point and the transport properties of ILs such as conductivity and viscosity. The hypotheses outlined above are tested with respect to a range of *N*-methyl-*N*-alkyl pyrrolidinium ($C_n$mpyr) and *N*-methyl-*N*-alkyl imidazolium ($C_n$mim) salts for which experimental data were available.

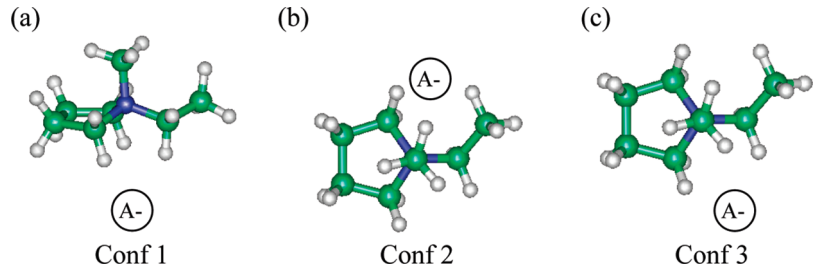

Figure 1. Ion-pair conformations of [$C_n$mpyr][A] salts.

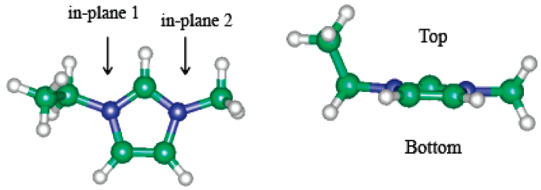

Figure 2. Ion-pair conformations of [$C_n$mim][A] salts.

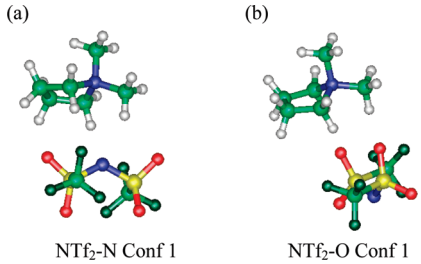

Figure 3. Interaction modes for the NTf_2 anion.

Anions represented in the study include: Br^-, BF_4^-, PF_6^-, $N(CN)_2^-$, $N(SO_2CF_3)_2^-$ (also known as NTf_2^-), mesylate, and tosylate.

Theoretical Procedures

Standard molecular orbital calculations were performed using Gaussian 09.[36] Details on the geometry optimizations and calculations of IPBE are given below.

Geometry Optimizations. A full conformational search was performed on each individual anion and cation to obtain the structures of lowest energy. With respect to the alkyl chains on the cations, it was observed that for ethyl, propyl, and butyl chains, the linear chain was always the lowest in energy. Therefore, for alkyl chains longer than butyl, where the number of conformations is quite large, extra alkyl groups were added to the terminal carbon in a linear arrangement.

The optimized lowest energy structures of the individual ions were used to construct ion pairs, which formed the starting points for the optimizations of the ion pairs. Different modes of cation−anion interaction were considered to identify the lowest energy conformations. For $C_n$mpyr salts, three possible locations of the anion around the cation, as shown in Figure 1, were considered. For $C_n$mim salts, a previous study identified seven possible locations for the anion around the cation.[37] Only the four positions shown in Figure 2 were considered in this project; other positions were excluded because they were significantly higher in energy. For NTf_2^-, both monodentate N coordination and bidentate O−O coordination were considered. (See Figure 3.) $N(CN)_2^-$, which is analogous in structure to NTf_2^-, also has two potential modes of interaction, and both interaction modes were considered.

All geometry optimizations were carried out at the B3LYP/6-31+G(d) level of theory with tight convergence criteria. This level of theory is considered to be reliable for predicting structures and is routinely used for geometry optimizations. Optimized structures were confirmed to be minima by frequency analysis.

Calculation of Ion-Pair Binding Energy. IPBE was calculated using the minimum-energy geometries of the individual cations and ions and corresponding ion pairs

$$\mathrm{IPBE} = E_{\mathrm{ion-pair}} - (E_{\mathrm{cation}}^{\mathrm{min}} + E_{\mathrm{anion}}^{\mathrm{min}}) + \Delta\mathrm{ZPVE} \quad (5)$$

Total IPBEs were calculated at the MP2/6-311+G(3df,2p) level and were also counterpoise-corrected using the Boys and Bernardi approach.[38] IPBEs include scaled zero-point vibrational energies (ZPVEs).[39] It has previously been established that this level of theory is reliable for calculating trends in IPBE for the types of systems included in this study.[40] In the first approximation, the Hartree−Fock (HF) energy could be considered to be the electrostatic component of the IPBE. The difference between the MP2 and HF energies represents the contribution from electron correlation effects and was taken as the dispersion component of the IPBE, and thus the dispersion component accounts for all electron correlation effects, including polarization and induction.

Results and Discussion

The experimental data against which IPBEs are compared were taken from the literature. (See the Supporting Information for further details.)

Melting Point. Experimental melting points of pyrrolidinium- and imidazolium-based ILs show a distinctive trend with increasing alkyl chain length. (See Figure 4.) For short alkyl chains, the melting point decreases with increasing alkyl chain length because of increased shielding of the charge on the cation. For long alkyl chains, the melting point increases with increasing alkyl chain length because of increased dispersion interactions between alkyl chains on neighboring cations. MD simulations[41] and crystallographic studies[42] provide evidence of the dominance of the alkyl chain interactions for ILs containing cations with long alkyl chains. The IPBE does not include these dispersion interactions between alkyl chains on cations, which dominate the interionic interactions of the ILs once the melting point starts to increase. Therefore, the correlations with melting point presented in this study are confined to salts for which the melting point is still decreasing with alkyl chain length.

According to the hypothesis set out above, the ratio of total IPBE to its dispersion component should correlate with melting point. For convenience, further in the text this ratio is referred to as "the ratio".

Trends with increasing alkyl chain length on the cation are shown in Figure 5. In this plot, each series represents a particular anion, and each data point in the series corresponds to a different alkyl chain length on the cation. As indicated by the linear

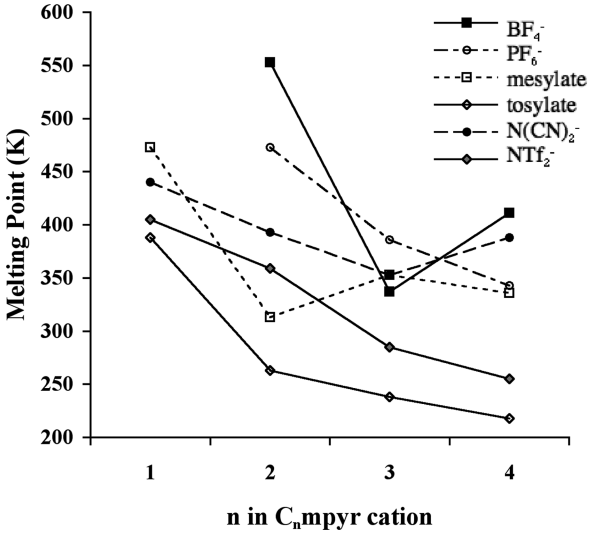

Figure 4. Trends in melting point with increasing alkyl chain length for $C_n$mpyr salts.

trends, the ratio generally correlates well with the melting point, and no obvious correlation was found between the IPBE and the melting point. There are, however, some exceptions. For [$C_n$mim][Br], the ratio for the top conformation, which was the lowest energy structure, does not show any correlation with melting point; however, the ratio for the in-plane conformation did show a similar correlation to that observed for the other salts. These two conformations are very close in energy (<6 kJ mol^{-1} apart); therefore, it is likely that both conformations exist in the salt simultaneously. The Boltzmann distribution, indicating the relative proportions of different ion-pair conformations at a given temperature, might need to be considered to obtain a weighted average of the IPBEs that accounts for all possible conformations of the ion pair to produce better correlations.

The ratios for [$C_n$mim][NTf_2] were generally consistent with results for the $C_n$mpyr salts. For [$C_n$mim][Br], the top conformation seems more consistent with the results for the $C_n$mpyr salts than the in-plane conformation. However, multiple ion-pair effects need to be considered for imidazolium salts because the $C_n$mim cation is aromatic and $\pi-\pi$ stacking interactions between cations may be significant for some imidazolium-based salts.[43] These $\pi-\pi$ stacking interactions would add to the dispersion component of the lattice energy, and thus taking this additional contribution and the Boltzmann average of the IPBEs for both the in-plane and top conformations might move the ratio of [$C_n$mim][Br] toward the $C_n$mpyr data points.

For trends across different types of anions, the ratio was found to correlate better than the total IPBE with melting points. An illustrative example is the trends observed for the C_2mpyr cation shown in Figure 6. The two outliers are the N-coordinated NTf_2 conformation and mesylate. In the case of NTf_2, the O-coordinated conformation fits the trend. As noted above, this suggests the importance of considering all possible ion-pair conformations, not just the lowest energy one. In the case of mesylate, [C_2mpyr][mesylate] is at the turning point where melting point starts to increase with alkyl chain length and dispersion interactions between alkyl chains on the cations start to dominate in determining the melting point. As noted above, the proposed correlation is limited to cases where the cation−anion interaction dominates the lattice energy of the salt.

To sum up, a linear correlation is observed between the proposed ratio of the total IPBE to its dispersion component and melting point, particularly when considering trends for individual anions, indicating the anion dependence of the melting point in ILs. However, it is important to note a number of limitations. Because the ratio is based on the IPBE, it will only be able to predict trends where the thermodynamic properties are dominated by cation−anion interactions, that is, when other short-range interactions (e.g., van der Waals interactions between long alkyl chains in cations) contribute only marginally to the lattice energy. Where multiple configurations of the cation−anion pairs of similar energy exist, it may be necessary to account for conformations other than the lowest energy one, taking into account the Boltzmann average of their IPBEs at a given temperature.

Transport Properties. According to the second hypothesis set out above, the dispersion component of the IPBE correlates with transport properties such as conductivity and viscosity. Transport properties of $C_n$mpyr and $C_n$mim salts that lie close to the ideal line on the Walden plot (Figure 7) were considered here.

Previously, in our group, we showed that the deviation from the ideal line on the Walden plot (ΔW) correlated with IPBE for phosphonium-based ionic liquids.[29] For the $C_n$mim and $C_n$mpyr salts studied in this work, no obvious correlation was

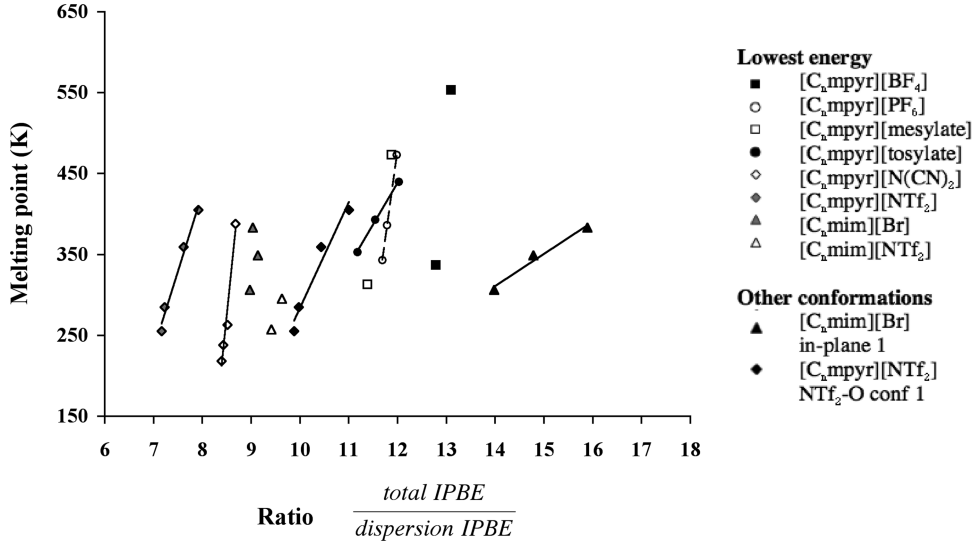

Figure 5. Correlation of ratio with melting point across cations.

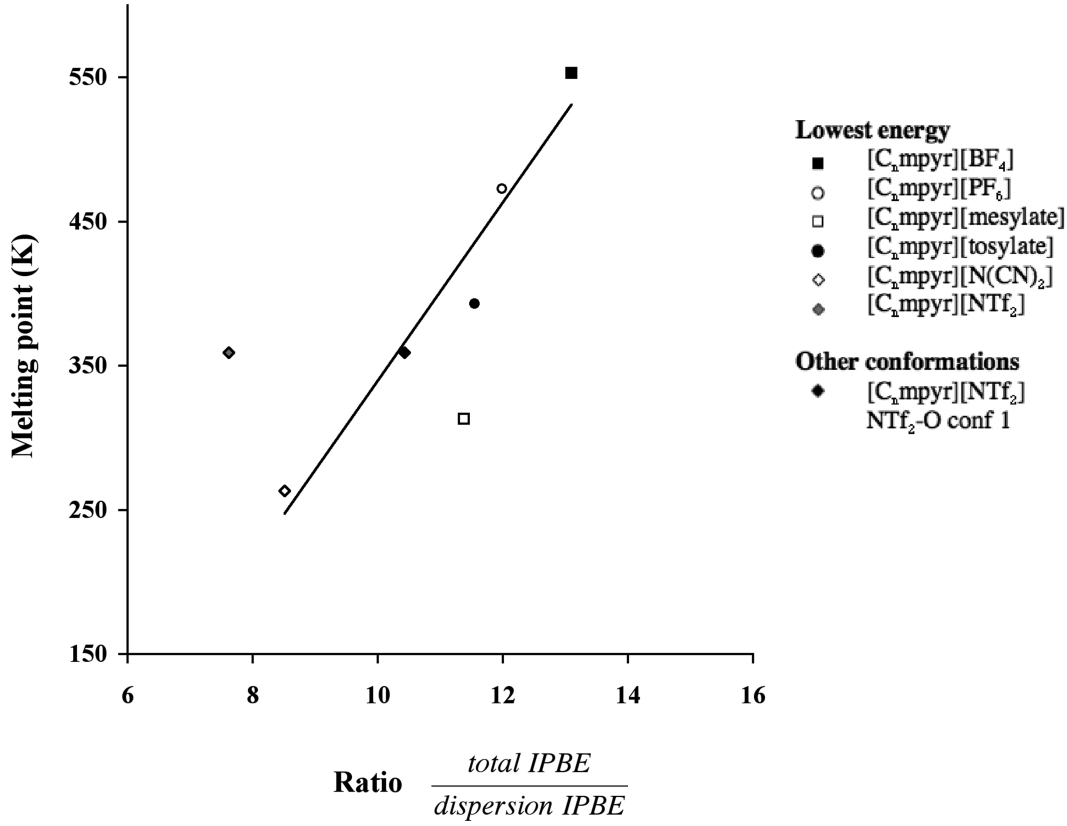

Figure 6. Correlation of the ratio with melting point across anions for C_2mpyr salts.

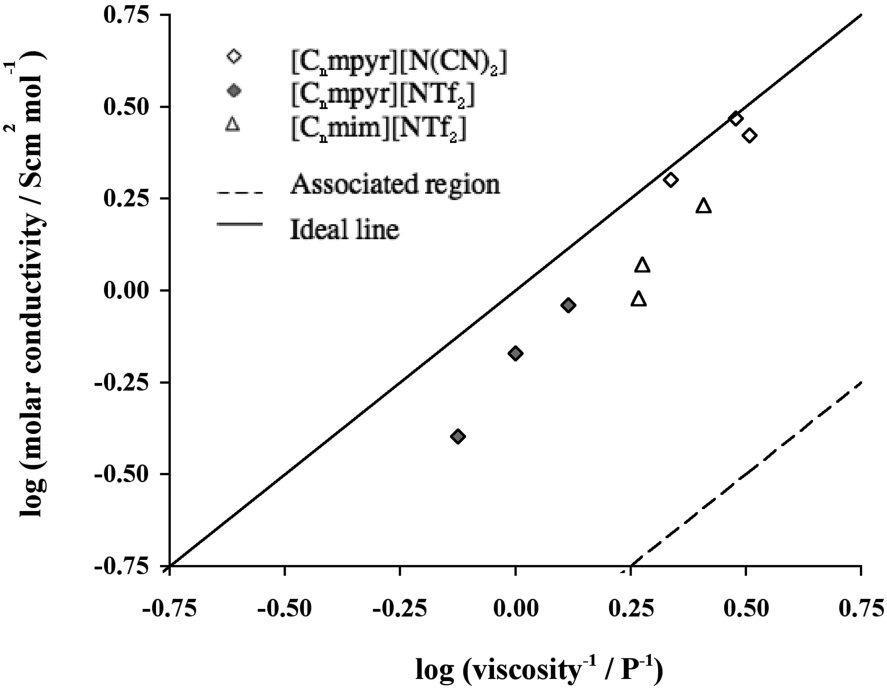

Figure 7. Walden plot for $C_n$mpyr and $C_n$mim salts.

observed between total IPBEs and ΔW. This is not necessarily inconsistent with the previous study. Phosphonium-based salts lie in the so-called associated region of the Walden plot, which implies a strong association of ions, including ion pairing. The combination of low conductivities and low viscosities of phosphonium salts was explained by the fact that cations and anions were strongly paired, with few interactions between ion pairs. In that case, a smaller IPBE would make ion pairs easier to separate, producing higher conductivities and smaller ΔW. ILs studied here lie very close to the ideal line; therefore, there may be no significant long-lived ion pairs that could significantly reduce conductivity.[44] As a result, no correlation between total IPBE and ΔW for ILs with the close-to-ideal behavior on the Walden plot is expected.

In this study, it was found that the dispersion component of IPBE correlated better with viscosities and conductivities (Figures 8 and 9) than the total IPBE or its electrostatic component. We suggest that the dispersion component (and not

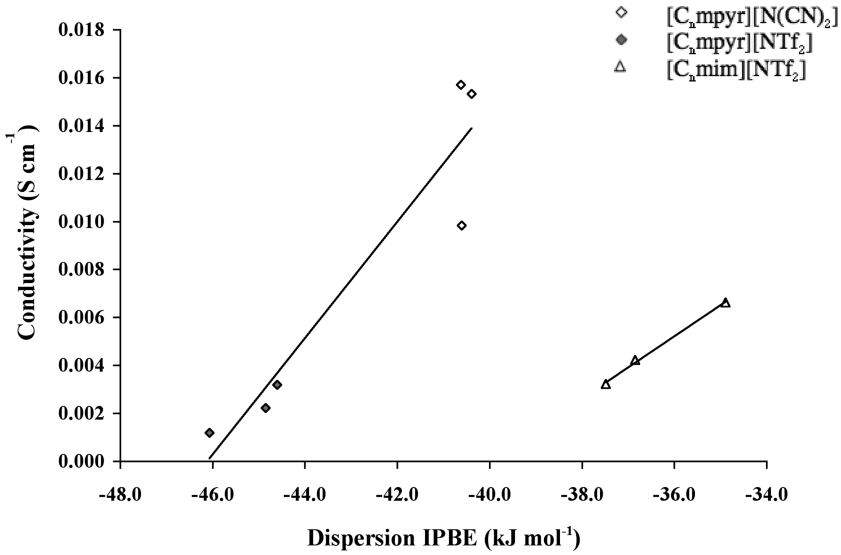

Figure 8. Correlation of dispersion component of IPBE with conductivity for global minimum ion-pair conformation.

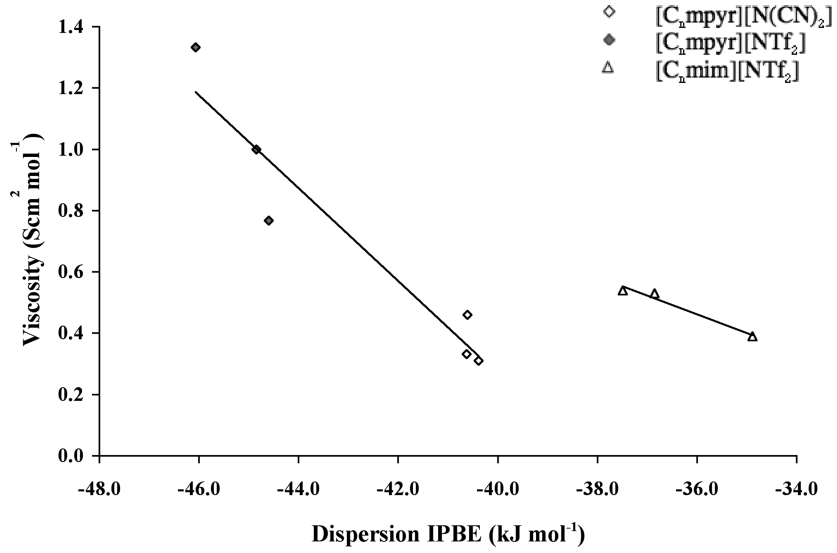

Figure 9. Correlation of dispersion component of IPBE with viscosity for global minimum ion-pair conformation.

IPBE itself) correlates with conductivity and viscosity because of the fact that short-range dispersion interactions are first to be disrupted to allow ions to move. Stronger long-range electrostatic interactions may remain approximately constant as the ions move; for example, as one anion moves away from a cation, another anion may approach the cation so that the electrostatic interaction the cation experiences does not change significantly as a result of the motion. Dispersion interactions are much shorter range and rely on instantaneous dipole moments created in nearby electron clouds, and the motion of the ions may diminish these interactions quite substantially.

In Figures 8 and 9, C$_n$mpyr and C$_n$mim salts form separate trend lines. Interestingly, the slopes of the C$_n$mpyr and C$_n$mim trend lines are relatively similar. The slightly greater slopes for C$_n$mpyr salts, which are more apparent for viscosity, suggest that dispersion interactions have a more significant effect on the transport properties of C$_n$mpyr ILs than on the transport properties of C$_n$mim ILs. The shift between the C$_n$mpyr and C$_n$mim trend lines may be attributable to additional $\pi-\pi$ stacking interactions between C$_n$mim cations, which are not included in the IPBE.

In summary, it was observed that the dispersion component of the IPBE correlates better than total IPBE or its electrostatic component with transport properties such as conductivity and viscosity. C$_n$mpyr and C$_n$mim salts form distinct trend lines with similar slopes. The gap between the linear trends might possibly be attributed to $\pi-\pi$ stacking interactions between C$_n$mim cations.

Conclusions

Separation of electrostatic and dispersion components of the total IPBE leads to good correlations with melting points and transport properties of ILs such as conductivity and viscosity. A linear correlation is observed between melting point and the ratio of total IPBE to its dispersion component, particularly when considering trends for individual anions, indicating the anion dependence of the melting point in ILs. The results of this study also suggest that the inclusion of contributions from all possible ion-pair conformations close in energy to the lowest energy conformation through the Boltzmann average of their IPBEs at a given temperature might improve the established correlations. A linear correlation is also observed between the dispersion component of the IPBE and transport properties such as conductivity and viscosity. C$_n$mpyr and C$_n$mim salts that have close-to-ideal behavior on the Walden plot form distinct linear

trends with similar slopes. In summary, the current study highlights the importance of accurate calculations of dispersion interactions due to electron correlation and hence the need to use quantum chemical methods that properly treat dispersion interactions for accurate predictions of thermodynamic and transport properties of ILs.

An important limitation of using the binding energy of a single ion pair to predict thermodynamic and transport properties involving the solid and liquid states is that it does not account for short-range cation−cation and anion−anion interactions. Therefore, our proposed correlation between the ratio of the total IPBE and its dispersion component with melting point is not expected to hold for ionic forming organic salts dominated by these short-range interactions (e.g., alkyl−alkyl chain interactions between cations or $\pi-\pi$ stacking interactions between anions). To account for same-charge interactions, large-scale ab initio calculations (i.e., systems containing multiple ion pairs) of ionic liquids are currently underway, thus paving the way toward the fully ab intio MD approach that will enable accurate predictions of thermodynamic and transport properties of ionic liquids at a given temperature.

To further test the hypotheses outlined in this article, a more comprehensive study on a larger group of ILs, using more accurate theoretical methods to separate electrostatic and dispersion components of the IPBE is currently in progress.

Acknowledgment. We gratefully acknowledge generous allocations of computing time from the National Facility of the National Computational Infrastructure (Canberra, Australia) and the Monash Sun Grid Cluster at the e-research centre of Monash University. E.I.I. and D.R.M. acknowledge the support of the Australian Research Council for their Fellowships.

Supporting Information Available: Melting points, conductivities, and viscosities. This material is available free of charge via the Internet at http://pubs.acs.org.

References and Notes

(1) Katritzky, A. R.; Lomaka, A.; Petrukhin, R.; Jain, R.; Karelson, M.; Visser, A. E.; Rogers, R. D. *J. Chem. Inf. Comput. Sci.* **2002**, *42*, 71–74.

(2) Marsh, K. N.; Boxall, J. A.; Lichtenthaler, R. *Fluid Phase Equilib.* **2004**, *219*, 93–98.

(3) Park, S.; Kazlauskas, R. J. *Curr. Opin. Biotechnol.* **2003**, *14*, 432–437.

(4) de Souza, R. F.; Padilha, J. C.; Gonclaves, R. S.; Dupont, J. *Electrochem. Commun.* **2003**, *5*, 728–731.

(5) Kuang, D.; Wang, P.; Ito, S.; Zakeeruddin, S. M.; Gratzel, M. *J. Am. Chem. Soc.* **2006**, *128*, 7732–7733.

(6) Shin, J.-H.; Henderson, W. A.; Scaccia, S.; Prosini, P. P.; Passerini, S. *J. Power Sources* **2006**, *156*, 560–566.

(7) Eike, D. M.; Brennecke, J. F.; Maginn, E. J. *Green Chem.* **2003**, *5*, 323–328.

(8) Katritzky, A. R.; Jain, R.; Lomaka, A.; Petrukhin, R.; Karelson, M.; Visser, A. E.; Rogers, R. D. *J. Chem. Inf. Comput. Sci.* **2002**, *42*, 225–231.

(9) Trohalaki, S.; Pachter, R.; Drake, G. W.; Hawkins, T. *Energy Fuels* **2005**, *19*, 279–284.

(10) Gardas, R. L.; Coutinho, J. A. P. *AIChE J.* **2009**, *55*, 1274–1290.

(11) Gardas, R. L.; Ge, R.; Goodrich, P.; Hardacre, C.; Hussain, A.; Rooney, D. W. *J. Chem. Eng. Data* **2010**, *55*, 1505–1515.

(12) Alavi, S.; Thompson, D. L. *J. Chem. Phys.* **2005**, *122*, 154704.

(13) Jayaraman, S.; Maginn, E. J. *J. Chem. Phys.* **2007**, *127*, 214504.

(14) Koddermann, T.; Paschek, D.; Ludwig, R. *ChemPhysChem* **2007**, *8*, 2464–2470.

(15) Santos, L. M. N. B. F.; Lopes, J. N. C.; Coutinho, J. A. P.; Esperanca, J. M. S. S.; Gomes, L. R.; Marrucho, I. M.; Rebelo, L. P. N. *J. Am. Chem. Soc.* **2007**, *129*, 284–285.

(16) Kelkar, M. S.; Maginn, E. J. *J. Phys. Chem. B* **2007**, *111*, 4867–4876.

(17) Logotheti, G.; Ramos, J.; Economou, I. G. *J. Phys. Chem. B* **2009**, *113*, 7211–7224.

(18) Borodin, O.; Smith, G. D. *J. Phys. Chem. B* **2006**, *110*, 11481–11490.

(19) Hunt, P. *Mol. Simul.* **2006**, *32*, 1–10.

(20) Maginn, E. J. *Acc. Chem. Res.* **2007**, *40*, 1200–1207.

(21) Kelkar, M. S.; Maginn, E. J. *J. Phys. Chem. B* **2007**, *111*, 9424–9427.

(22) Ghatee, M. H.; Ansari, Y. *J. Chem. Phys.* **2007**, *126*, 154502.

(23) Zahn, S.; Thar, J.; Kirchner, B. *J. Chem. Phys.* **2010**, *132*, 124506.

(24) Ludwig, R. *Phys. Chem. Chem. Phys.* **2008**, *10*, 4333–4339.

(25) Izgorodina, E. I.; Forsyth, M.; MacFarlane, D. R. *Aust. J. Chem.* **2007**, *60*, 15–20.

(26) Zahn, S.; Uhlig, F.; Thar, J.; Spickermann, C.; Kirchner, B. *Angew. Chem., Int. Ed.* **2008**, *47*, 3639–3641.

(27) Turner, E. A.; Pye, C. C.; Singer, R. D. *J. Phys. Chem. A* **2003**, *107*, 2277–2288.

(28) Tsuzuki, S.; Tokuda, H.; Hayamizu, K.; Watanabe, M. *J. Phys. Chem. B* **2005**, *109*, 16474–16481.

(29) Fraser, K. J.; Izgorodina, E. I.; Forsyth, M.; Scott, J. L.; MacFarlane, D. R. *Chem. Commun.* **2007**, 3817–3819.

(30) Hunt, P. A. *J. Phys. Chem. B* **2007**, *111*, 4844–4853.

(31) Hunt, P. A.; Gould, I. R.; Kirchner, B. *Aust. J. Chem.* **2007**, *60*, 9–14.

(32) Slattery, J. M.; Daguenet, C.; Dyson, P. J.; Schubert, T. J. S.; Krossing, I. *Angew. Chem., Int. Ed.* **2007**, *46*, 1–6.

(33) Krossing, I.; Slattery, J. M.; Daguenet, C.; Dyson, P. J.; Oleinikova, A.; Weingartner, H. *J. Am. Chem. Soc.* **2006**, *128*, 13427–13434.

(34) Glasser, L.; Jenkins, D. B. *Chem. Soc. Rev.* **2005**, *34*, 866–874.

(35) Izgorodina, E. I.; Bernard, U. L.; Dean, P. M.; Pringle, J. M.; MacFarlane, D. R. *Cryst. Growth Des.* **2009**, *9*, 4834–4839.

(36) Frisch, M. J.; Trucks, G. W.; Schlegel, H. B.; Scuseria, G. E.; Robb, M. A.; Cheeseman, J. R.; Montgomery, J. A.; Jr., Vreven, T.; Kudin, K. N.; Burant, J. C.; Millam, J. M.; Iyengar, S. S.; Tomasi, J.; Barone, V.; Mennucci, B.; Cossi, M.; Scalmani, G.; Rega, N.; Petersson, G. A.; Nakatsuji, H.; Hada, M.; Ehara, M.; Toyota, K.; Fukuda, R.; Hasegawa, J.; Ishida, M.; Nakajima, T.; Honda, Y.; Kitao, O.; Nakai, H.; Klene, M.; Li, X.; Knox, J. E.; Hratchian, H. P.; Cross, J. B.; Bakken, V.; Adamo, C.; Jaramillo, J.; Gomperts, R.; Stratmann, R. E.; Yazyev, O.; Austin, A. J.; Cammi, R.; Pomelli, C.; Ochterski, J. W.; Ayala, P. Y.; Morokuma, K.; Voth, G. A.; Salvador, P.; Dannenberg, J. J.; Zakrzewski, V. G.; Dapprich, S.; Daniels, A. D.; Strain, M. C.; Farkas, O.; Malick, D. K.; Rabuck, A. D.; Raghavachari, K.; Foresman, J. B.; Ortiz, J. V.; Cui, Q.; Baboul, A. G.; Clifford, S.; Cioslowski, J.; Stefanov, B. B.; G. Liu, A. L.; Piskorz, P.; Komaromi, I.; Martin, R. L.; Fox, D. J.; Keith, T.; Al-Laham, M. A.; Peng, C. Y.; Nanayakkara, A.; Challacombe, M.; Gill, P. M. W.; Johnson, B.; Chen, W.; Wong, M. W.; Gonzalez, C.; Pople, J. A. *GAUSSIAN 09*, revision A.02; Gaussian, Inc.: Wallingford, CT, 2009.

(37) Hunt, P. A.; Kirchner, B.; Welton, T. *Chem.—Eur. J.* **2006**, *12*, 6762–6775.

(38) Boys, S. F.; Bernardi, F. *Mol. Phys.* **1970**, *19*, 553–566.

(39) Scott, A. P.; Radom, L. *J. Phys. Chem.* **1996**, *100*, 16502–16513.

(40) Izgorodina, E. I.; Bernard, U. L.; MacFarlane, D. R. *J. Phys. Chem. A* **2009**, *113*, 7064–7072.

(41) Shimizu, K.; Tariq, M.; Gomes, M. F. C.; Rebelo, L. P. N.; Lopes, J. N. C. *J. Phys. Chem. B* **2010**, *114*, 5831–5834.

(42) Dibrov, S. M.; Kochi, J. K. *Acta Crystallogr.* **2006**, *C62*, o19–o21.

(43) Li, H.; Boatz, J. A.; Gordon, M. S. *J. Am. Chem. Soc.* **2008**, *130*, 392–393.

(44) MacFarlane, D. R.; Forsyth, M.; Izgorodina, E. I.; Abbott, A. P.; Annat, G.; Fraser, K. *Phys. Chem. Chem. Phys.* **2009**, *11*, 4962–4967.

JP1048875